Journal of Nuclear Medicine, published on September 9, 2021 as doi:10.2967/jnumed.121.262506

Glucagon Like Peptide-1 receptor imaging in individuals with Type 2 Diabetes

Short title: GLP1R imaging in T2D

Authors: Olof Eriksson[1,2*], Irina Velikyan[3,4], Torsten Haack[5], Martin Bossart[5], Iina Laitinen[6], Philip J Larsen[7], Jan Erik Berglund[8], Gunnar Antoni[3,4], Lars Johansson[1], Stefan Pierrou[1], Joachim Tillner[9], Michael Wagner[5*]

Affiliations:

1. Antaros Medical AB, Uppsala, Sweden
2. Science for Life Laboratory, Department of Medicinal Chemistry, Uppsala University, Uppsala, Sweden
3. Department of Medicinal Chemistry, Uppsala University, Uppsala, Sweden
4. Akademiska Sjukhuset, Uppsala, Sweden
5. R&D Research Platform, Integrated Drug Discovery, Sanofi, Frankfurt, Germany
6. Global Imaging, Sanofi, Frankfurt, Germany; current address: Antaros Medical AB, Uppsala, Sweden
7. Diabetes Research, Sanofi, Frankfurt, Germany; current address: Bayer Pharmaceuticals, Wuppertal, Germany
8. Clinical Trial Consultants AB, Uppsala, Sweden
9. Translational Medicine, Sanofi, Frankfurt, Germany

*Corresponding authors:
Olof Eriksson
Antaros Medical AB
Uppsala Science Park
Dag Hammarskjölds Väg 14C, 3tr
SE-751 83 Uppsala, SWEDEN
(c): +46-707903054
(e): olof.eriksson@antarosmedical.com

Michael Wagner
Sanofi-Aventis Deutschland GmbH
Industriepark Hoechst, Building G838
D-65926 Frankfurt am Main, Germany
(c): +49 69 305 4875
(e): Michael.Wagner@sanofi.com

Word count: 3380
Figures: 4
Tables: 3
ClinicalTrials.gov: NCT03350191

Keywords: GLP1R, PET, Exendin, type 2 diabetes, beta cell mass

ABSTRACT

Introduction: The Glucagon Like Peptide-1 receptor (GLP1R) is a gut hormone receptor, intricately linked to regulation of blood glucose homeostasis via several mechanisms. It is an established and emergent drug target in metabolic disease. Positron Emission Tomography (PET) radioligand ^{68}Ga-DO3A-VS-Exendin4 (^{68}Ga-Exendin4) has the potential to enable longitudinal studies of the GLP1R in human pancreas.

Methods: ^{68}Ga-Exendin4 PET/CT examinations were acquired in overweight to obese individuals with type 2 diabetes (T2D) (n=13) as part of a larger target engagement study (NCT03350191). A scanning protocol was developed to optimize reproducibility (target amount of 0.5 MBq/kg, corresponding to <0.2µg/kg peptide, blood sampling and tracer stability assessment). Pancreas and abdominal organs were segmented and binding was correlated to clinical parameters.

Results: The pancreatic uptake of ^{68}Ga-Exendin4, but not in other abdominal tissues, was high but variable between individuals. There was no evidence of self-blocking of the GLP1R by the tracer in this protocol, despite the high potency of Exendin4. The results show that a full dynamic scan can be simplified to a short static scan, potentially increasing throughput and reduce patient discomfort. ^{68}Ga-Exendin4 concentration in pancreas (i.e. GLP1R density) correlated inversely with the age of the individual, and had a tendency to correlate positively to BMI. However, the total GLP1R content in pancreas did not.

Conclusion: In summary, we present an optimized and simplified ^{68}Ga-Exendin4 scanning protocol, to enable reproducible imaging of the GLP1R in pancreas. ^{68}Ga-Exendin4 PET may enable quantification of longitudinal changes of pancreatic GLP1R during the development in T2D, as well as target engagement studies of novel GLP-1 agonists.

INTRODUCTION

The Glucagon Like Peptide-1 (GLP-1) receptor (GLP1R) is a gut hormone receptor, intricately linked to regulation of blood glucose homeostasis via several mechanisms such as insulin secretion, gastric emptying and control of food intake (*1*). Endogenous GLP-1 peptide is released from the intestinal L-cells in response to nutrient intake. Synthetic GLP-1 agonists are already approved for treatment of e.g. type 2 diabetes (T2D), and further insight into their mechanism of action is still of utmost interest. Several recent studies have demonstrated beneficial effects of GLP-1 agonists on HbA1c, cardiac function and survival (*2,3*).

Exendin-4 is a synthetic peptide, which binds to GLP1R with nanomolar affinity and high specificity (*4*). The development of Gallium-68 radiolabeled analogues of Exendin4 (*5,6*) have recently enabled non-invasive Positron Emission Tomography (PET) imaging in humans, primarily for the diagnosis and localization of insulinomas (*7,8*), as well as expression of GLP1R in the pancreas.

The possibility of longitudinal imaging to quantify GLP1R density in the pancreas is of interest both in the context of assessment of drug mechanism of action (e.g. in the context of unimolecular dual and trigonal agonists) (*9,10*), as well as due to the potential association between GLP1R expression and the remaining beta cell mass (*11*). Here, we employed ^{68}Ga-DO3A-VS-Exendin4 (^{68}Ga-Exendin4) for PET imaging of GLP1R in the human pancreas. The current study was performed as part of a clinical trial investigating the target engagement of a novel GLP1/glucagon receptor dual agonist SAR425899 in individuals with T2D (ClinicalTrials.gov: NCT03350191) (*12*).

Here, we demonstrate for the first time the non-invasive quantification of GLP1R density in the pancreas in individuals with T2D by PET imaging. We furthermore outline a protocol for reproducible, longitudinal and accurate ^{68}Ga-Exendin4 PET/CT scanning, and explore the origin of the variability of pancreatic GLP1R density in the pancreas in this patient population.

METHODS AND MATERIALS

Non-human primate PET study

A ^{68}Ga-Exendin4 PET/CT imaging study in healthy cynomolgus non-human primates (NHPs) was in part reported and described in detail previously (*5*). Briefly, NHPs were scanned by ^{68}Ga-Exendin4 PET using a dose escalation study design, where several examinations were performed, several hours apart, over the course of one or several experimental days. Each subsequent scan entailed higher peptide mass and radioactive dose, to minimize influence from the preceding scan (See Table 1 for details). The resulting data set enables analysis of the self-blocking effect of the increasing amounts of co-injected unlabelled Exendin4 precursor peptide.

Previously, only the simplified SUV analysis of n=3 of the NHPs (n=8 scans) was reported (*5*). To better understand the peptide doses where self-blocking starts to occurs, in preparation for the design of the clinical study, we re-analysed the dynamic NHP data from all n=12 scans by graphical analysis using an image derived blood plasma input.

Pancreas and other tissues of interest (such as spleen as a negative reference tissue) was delineated using PMOD 4.0 (PMOD Technologies, Zürich, Switzerland). The PET signal for each tissue and time frame was corrected for the injected amount and the image derived input function (IDIF) was extracted by segmenting voxels fully within the lumen of aorta descendant as identified on early PET frames and co-registered CT projections. The aorta signal was further corrected for the plasma partition.

The volume of distribution (V_t) of ^{68}Ga-Exendin4 in pancreas was estimated by graphical analysis according to Logan using the IDIF as input using the PMOD PKIN module (*13*). Patlak graphical analysis was also attempted (*14*), assuming irreversible uptake of ^{68}Ga-Exendin4 in tissue due to receptor agonism and internalization, but this model failed in some individuals and is not reported.

The pancreatic V_t for each scan was plotted against the amount of co-injected unlabeled precursor peptide to explore the self-blocking at different doses.

Furthermore, the pancreatic V_t was plotted against the static uptake values at different time points, to determine if static Standardized Uptake Values (SUV) values could replace full dynamic PET scans with invasive plasma sampling.

Clinical study design

These ^{68}Ga-Exendin4 PET/CT examinations were acquired as part of a phase Ib, single center, open-label study assessing the GCGR and GLP1R occupancy of dual agonist SAR425899 in overweight to obese T2D patients (ClinicalTrials.gov: NCT03350191). Individuals with T2D (n=13) were recruited and underwent PET/CT scanning for the GLP1R availability in pancreas (^{68}Ga-Exendin4) and glucagon receptor availability in liver (^{68}Ga-DO3A-VS-Tuna-2) at baseline. Participants were then treated with up to 0.12 or 0.2 mg SAR425899 daily from three weeks, followed by on-drug scanning with ^{68}Ga-Exendin4 and ^{68}Ga-DO3A-VS-Tuna-2. Six participants completed the full study, and the results from those individuals, especially the occupancy of SAR425899 as evaluated by PET, were previously reported (*12*). This study reports the results of all the n=13 baseline ^{68}Ga-Exendin4 PET scans and the details of the procedures. The baseline examination of the n=13 ^{68}Ga-DO3A-VS-Tuna-2 examinations was similarly reported independently (*15*).

Patient population

Overweight to obese individuals diagnosed with T2D (n=13) were recruited to the study. The participants had a median age of 69 years (range 50-76), a mean BMI of 31.2±3.0 kg/m^2. Of the n=13 participants, n=12 were males and n=1 was female. Patients were not allowed to be on any antidiabetic medication during the study except for stable metformin and/or sulfonylurea treatment.

No control group with non-diabetic individuals was included, since the full study was aimed at assessing drug efficacy and occupancy, and thus included three weeks of drug treatment with SAR425899.

All study participants provided written informed consent. Study protocols were approved by National Health Authorities and an Independent Ethics Committee and the trial was performed in accordance with the guidelines established by the Declaration of Helsinki and the International Conference on Harmonization - Good Clinical Practice.

PET/CT examinations

Good Manufacturing Practise (GMP) DO3A-Exendin-4 was provided by Sanofi. GMP quality ^{68}Ga-Exendin4 was produced on an automated synthesizer (Modular Lab

Pharm Tracer, Eckert & Ziegler, Germany) as developed and reported previously (*12*,*16*). The radiochemical purity was over 90% with no unknown single impurity of over 5%.

The PET assessments were performed 3 h after a standardized meal followed by fasting, to minimize the variability of GLP-1 levels at the time of the scanning. The individuals were examined over the abdomen with a Discovery MI PET/CT scanner (20 cm FOV, GE Healthcare, Milwaukee, MI, USA). A low dose CT was performed for attenuation correction and anatomical co-registration of PET images. The dose of the CT was limited by dosimetry considerations, given each individual underwent up to four PET/CT examinations over the entire clinical study.

A target of 0.5 MBq/kg ^{68}Ga-Exendin4 (0.46±0.03 MBq/kg, corresponding to 0.14±0.04 µg/kg peptide) was administered intravenously as a bolus. The amount of administered ^{68}Ga-Exendin4 was based primarily on limiting the associated dose of DO3A-VS-Exendin4 precursor peptide to below 0.2µg/kg. This limit was imposed to minimize any self-block and the cut-off value was determined from the NHP dose escalation studies.

Dynamic PET was initiated at administration and continued for 60 minutes. Blood sampling for blood glucose was performed before and during the scan as a safety precaution as Exendin4 can stimulate insulin secretion at pharmacological doses. For three individuals, arterial sampling was performed 5, 30 and 60 min after ^{68}Ga-Exendin4 administration to measure the radioactivity in whole blood and plasma and to determine the metabolic stability of the tracer (see Supplementary data for methods).
PET images were reconstructed using an iterative VPFX-S algorithm (3 iterations, 3 subsets, matrix 256x256, Z-axis post-filter 3mm) with all relevant corrections performed (30 frames in total; 12 x 10 s, 6 x 30 s, 5 x 120 s, 5 x 300 s, 2 x 600 s).

PET image analysis

Abdominal tissues of interest, including pancreas (target tissue), aorta (input signal), kidney (excretion), spleen and erector spinae muscle (negative reference tissues) were manually segmented on co-registered PET/CT images using Carimas software v2.9 (Turku PET Center, Turku, Finland). The aorta was delineated by segmenting single voxels fully within the lumen of aorta descendant. The arterial plasma IDIF was generated by

correcting the aorta signal for plasma-to-whole blood partitioning and the percentage of intact ^{68}Ga-Exendin4 during the scan (based on a population estimate).

The kinetic data was fitted to different compartmental models and graphical analyses, including 1- and 2 tissue compartment models (1TC/ 2TC), Patlak and Logan analysis. Based on the fitting, performance and complexity of the models (Supplemental Tables 1-5), Patlak graphical analysis was selected as the optimal analysis method of the dynamic PET data. Furthermore, ^{68}Ga-Exendin4 triggers internalization in GLP1R positive tissues, leading to intracellular Gallium-68 trapping (Supplemental Figure 1A-B), theoretically fulfilling the irreversible binding criteria during the time of the scanning as assumed in Patlak analysis.The ^{68}Ga-Exendin4 net uptake rate (K_i) was estimated using Patlak graphical analysis in Excel (*14*).

K_i (mL/[mL*h]) was considered a measurement of the concentration of ^{68}Ga-Exendin4 binding in pancreas (likely proportional to the GLP1R density in pancreas). The total GLP1R content was thus estimated by multiplying K_i (mL/[mL*h]) by the pancreatic volume (mL) as segmented from the PET/CT images.

Statistics

Data on group level are reported as means±SD. Differences between groups were assessed by one-way ANOVA. Correlations were assessed by linear regression and Pearson's correlation coefficient (GraphPad Prism for Mac 8.0).

Data and resource availability statements

The data that support the findings of this study are available from Sanofi but restrictions apply to the availability of these data, which were used under license for the current study and therefore are not publicly available. Data are however available from the authors upon reasonable request and with permission of Sanofi.

RESULTS

Non-human primate PET dose escalation study

^{68}Ga-Exendin4 exhibited visually strong binding and high V_t in the pancreas at all scans co-injecting up to 0.2µg/kg unlabelled DO3A-VS-Exendin4 precursor peptide

(Figure 1A). There was a sharp decrease in binding already at peptide mass doses of 1µg/kg, while doses in excess of 10µg/kg reduced the pancreas binding to background. The dose inducing 50% decrease in binding (the "in vivo IC_{50}") was estimated to approximately 0.45µg/kg, indicating very high potency.

Binding was also estimated with a simple semi-quantitative SUV measurement of the pancreatic binding during the static time frame from 50-60 minutes post injection (SUV_{55min}). SUV_{55min} correlated strongly to V_t ($p<0.0001$, $r=0.96$) (Figure 1B).

Binding and biodistribution in individuals with T2D

^{68}Ga-Exendin4 was rapidly distributed in the abdominal tissues after intravenous administration (Figure 2A-B). Initially, the aorta and the left ventricle (i.e. blood signal) was clearly seen, followed by uptake in the pancreas, kidney and liver in the first 5 minutes. For the remaining duration of the scan (60 minutes), the increasing uptake in pancreas and kidney continued, while remaining tissues demonstrated clearance.

After 60 minutes, the uptake of ^{68}Ga-Exendin4 (assessed as SUV_{55min}) was clearly higher in pancreas compared to e.g. spleen, which has high perfusion comparable to pancreas, but is devoid of GLP1R (Figure 2C). There was a marked variability, almost 4-fold, in the magnitude of the pancreas uptake in different individuals (Figure 2C-D). Importantly, this variability was not reflected in other abdominal tissues or the blood signal, indicating it is not due to general differences in biodistribution or metabolism.

^{68}Ga-Exendin4 uptake was obvious in all three pancreatic segments caput (head), corpus (body) and cauda (tail), but tended to be higher in the cauda. However, separate delineation of the cauda was difficult due to potential spill-over from the kidney in some individuals.

Metabolic stability, self-block and protocol simplification

^{68}Ga-Exendin4 demonstrated high stability in blood after injection with more than 90% intact tracer in plasma 60 minutes after tracer administration (Table 2). ^{68}Ga-Exendin4 also exhibited high plasma partitioning (≈1.8) throughout the scan, i.e. most tracer was free in plasma available for distribution into tissue (Table 2). The net uptake rate

(K_i) of ^{68}Ga-Exendin4 in pancreas was calculated by Patlak graphical analysis, using the metabolite corrected arterial plasma curve as input (Table 3).

As per the study design, all individuals were administered less than 0.2µg/kg DO3A-VS-Exendin4 peptide to avoid self-blocking due to the high potency of the compound to GLP1R. As predicted, there was no negative correlation between the peptide mass dose and the net uptake rate, indicating that the self-block at these levels was negligible also in humans (Figure 3A).

The SUV_{55min} values correlated well with the net uptake rate (K_i) ($p<0.0001$, $r=0.92$), indicating that the long duration dynamic scanning and invasive blood sampling may be replaced by shorter static scanning from 50-60 minutes post tracer administration with only minor loss in accuracy (Figure 3B).

Binding correlation to age and BMI

As described above, there was a distinct variability in the ^{68}Ga-Exendin4 net uptake rate in pancreas. We therefore explored the potential correlation between ^{68}Ga-Exendin4 binding and patient characteristics and biometrics. The variability in ^{68}Ga-Exendin4 binding as assessed by K_i (i.e. GLP1R density) correlated negatively to the age of the participant ($p<0.05$, $r=-0.61$) (Figure 4A). The same correlation to age but using SUV_{55min} values was $r=-0.50$, $p=0.082$. Furthermore, there was a tendency for positive correlation between ^{68}Ga-Exendin4 binding in pancreas to the BMI of the participants ($p=0.064$, 5=0.53) (Figure 4B). Similarly, the correlation between BMI and SUV_{55min} values was $r=0.43$, $p=0.145$. However, when estimating the total ^{68}Ga-Exendin4 binding (i.e. total GLP1R content) by multiplying with the pancreas volume, no correlations remained (Figure 4C-D). The pancreatic volume of the participants ranged between 48-135 mL, and did not correlate to e.g. age or BMI in this cohort (Figure 5E-F).

DISCUSSION

In this study we demonstrate ^{68}Ga-Exendin4 binding and biodistribution in the pancreas of human individuals with T2D. Furthermore, we present an optimized and simplified ^{68}Ga-Exendin4 scanning protocol, based on these initial experiences.

Native Exendin4 is a highly potent GLP1R agonist, with subnanomolar potency (*17*). Radiolabeled ^{68}Ga-Exendin4 has excellent specificity for GLP1R (Supplementary Figure 1A) and affinity in the nanomolar range (*18*). In the absence of suitable antagonists, agonists such as Exendin4 can be utilized as PET tracers, but care must be taken to avoid unwanted pharmacological effects. We have previously demonstrated that ^{68}Ga-Exendin4 exhibits self-block also at low administered precursor peptide mass doses in NHP. Doses of around 0.5µg/kg elicits up to 50% blocking of the signal. This is not entirely unexpected, given its high potency for GLP1R. In fact peptide mass effects of similar magnitude were seen for two another gut hormone peptide PET tracers, ^{68}Ga-DO3A-VS-Tuna-2 (glucagon receptor agonist) and ^{68}Ga-S02-GIP-T4 (Glucose-Dependent Insulinotropic Polypeptide (GIP) receptor agonist), both with a potency in the pM range (*19,20*).

Here, we further demonstrate from NHP data that peptide mass effect can be avoided at doses of <0.2 µg/kg co-injected DO3A-VS-Exendin4. This influenced the design of the clinical study, which subsequently showed minimal mass effects. Thus, any future clinical studies with ^{68}Ga-Exendin4 should aim to administer no more than 0.2µg/kg precursor peptide. This limitation will likely entail optimized automated radiochemistry setup (*16*), since a molar activity of at least 20-30 MBq/nmol will be required. Furthermore, even at optimal molar activity, 0.2µg/kg will probably correspond to no more than 50-100 MBq to be administered – this in turn necessitates highly sensitive PET instrumentation for sufficient image quality.

Quantitative PET assessment usually entails quite complex correction of imaging data, including dynamic imaging acquisition of long duration, arterial sampling as well as metabolic stability measurement. Such complicated scanning protocols present logistical challenges as well as patient discomfort. Additionally, the analysis is time-consuming while requiring specialized software and expertise. Semi-quantitative measurements derived from static scanning protocols, such as Standardised Uptake Values (SUV), on the other hand, are simpler from the point of view of both the patient and the hospital, in addition to allowing for rapid analysis.

Both in the NHP and the clinical study, we could show that the static SUV value (SUV_{55min}) exhibited very strong correlation to the modelled parameter (which was derived from the full dynamic scanning protocol including blood sampling and metabolic stability correction of the input signal). Thus, it can be assumed that a shorted static scan 50-60 minutes post injection provides reasonable accuracy in assessment of GLP1R density in pancreas, with only minor loss in reproducibility as a full dynamic scan. In many cases this trade-off may be acceptable in order to substantially increase patient comfort and simplify scanning procedures and logistics. However, the correlation of ^{68}Ga-Exendin4 uptake as assessed by SUV_{55min} did not correlate as well to e.g. age as Patlak net uptake rate, indicating that the simplification of the analysis and scanning protocol may reduce power of the assessment.

A limitation of this study is the lack of a test-retest assessment, i.e. repeated scanning of the same subject without any intervention in between. Such data would provide important information of the reproducibility of the assessment either analyses by SUV_{55min} or Patlak net uptake rate. Unfortunately, test-retest scanning was not possible due to the full study design (ClinicalTrials.gov: NCT03350191) (12).

In short, future PET studies using ^{68}Ga-Exendin4 for assessment of GLP1R in pancreas should target to to co-inject less than 0.2µg/kg peptide. Moreover patient comfort and scanning throughput could be increased by limiting the scanning protocol to a static scan approximately 60 minutes after injection.

Despite the rigorous standardization of our scanning protocol, ^{68}Ga-Exendin4 exhibited a marked variability in pancreatic binding. We further explored potential reasons for this variability. There was a negative correlation to age in this material, indicating lower GLP1R density in pancreas of older individuals. A progressive decrease in GLP1R in the mouse brain has previously been reported (*21*). One of the major sources of ^{68}Ga-Exendin4 binding in the human pancreas is the beta cells, which exhibit strong GLP1R expression (*22*). The known decline of beta cell number and function with age (*23*) thus presents a possible mechanism for this reduction of ^{68}Ga-Exendin4 with increasing age.

However, when calculating the total GLP1R content (by multiplying ^{68}Ga-Exendin4 binding by the pancreas volume), the negative correlation did not prevail.

We also visually observe a general trend of higher ^{68}Ga-Exendin4 uptake in the cauda (tail) of the pancreas in many individuals. This is again interesting in the context of beta cells, since it has been demonstrated that the cauda exhibits approximately two-fold density of islets compared to the caput and the corpus (*24*). Thus, we observe several features of the ^{68}Ga-Exendin4 binding that is consistent with known beta cell distribution and function. Additionally, the large variability of ^{68}Ga-Exendin4 observed here (almost 4-fold) is in line with the large variability in beta cell mass seen in individuals with T2D as assessed by biopsy morphometric studies (*25*). More studies dedicated to this question are required to further establish the association between ^{68}Ga-Exendin4 binding and the beta cell mass in the human pancreas in T2D.

We observe a trend for a positive correlation between ^{68}Ga-Exendin4 binding and BMI in this cohort, i.e. increasing pancreatic GLP1R density correlated with higher BMI. It is difficult to assess if this is a reasonable observation, as there is limited data on the GLP1R density in the pancreas of obese subjects – likely due to the challenge of obtaining a diverse biopsy material of high quality, lack of reliable monoclonal antibodies for GLP1R as well as the time-consuming effort required for sectioning, staining and analyzing a sufficiently large data set to draw firm conclusions. Again, the correlation with BMI did not remain when estimating the total GLP1R content in the pancreas by multiplying with volume.

A limitation of the study and the correlations discussed above is the imbalanced gender distribution of the study population. Of n=13 included individuals, twelve were male and only a single female. The pancreatic binding in the female individuals was around the average in this cohort. However, the correlations seen here may only reflect the male population.

^{68}Ga-Exendin4 could conceivably serve as a biomarker for response to therapy. GLP-1 efficacy studies sometimes delineate sub groups of non-responding individuals and this is seen both in studies targeting populations with diabetes (*26*) and neurological disease (*27*). In this small material, some of the participants (n=7) completed 3 weeks up-titration with the dual GLP1/glucagon agonist SAR425899 and all responded to treatment with blood glucose lowering and weight reduction, regardless of exhibiting a wide range of GLP1R density in pancreas (*12*). Therefore, excessively up- or- down regulated GLP1R in the pancreas does not seem to predict GLP1 agonist responders or non-responders in this admittedly small cohort.

Conclusion

We present an optimized and simplified ^{68}Ga-Exendin4 scanning protocol, to enable reproducible imaging of the GLP1R in human pancreas. ^{68}Ga-Exendin4 PET may enable longitudinal quantification of changes in pancreatic GLP1R during the development in T2D, as well as target engagement studies of novel GLP-1 agonists.

ACKNOWLEGEMENTS

The clinical study was sponsored by Sanofi and performed in collaboration with Antaros Medical AB. The non-human primate study was sponsored by JDRF, Diabetesfonden and Barndiabetesfonden. Olof Erikssons position is funded by Science for Life Laboratory and the Swedish Research Council (2020-02312). We thank Eduard Kober, Hélène Savoye (both employed by Sanofi), and Mélanie Bovo (employed by Business France) for their support during the conduct and analysis of this study. We thank Ramkumar Selvaraju and Olle Korsgren for assistance during the conduct of the NHP study.

AUTHOR CONTRIBUTIONS

O.E. researched data, designed the study and wrote the manuscript. I.V. researched data and reviewed the manuscript. T.H. researched data and reviewed the manuscript. M.B. researched data and reviewed the manuscript. I.L. contributed to data analysis and reviewed the manuscript. PJ.L. researched data and reviewed the manuscript, J.E.B.

researched data and reviewed the manuscript. G.A. designed the study and reviewed the manuscript. L.J. designed the study and reviewed the manuscript. S.P. researched data and reviewed the manuscript. J.T. researched data, designed the study and reviewed the manuscript. M.W. designed the study and wrote the manuscript. O.E. is the guarantor of this work and, as such, had full access to all the data in the study and takes responsibility for the integrity of the data and the accuracy of the data analysis.

DISCLOSURES

Torsten Haack, Martin Bossart, Joachim Tillner, Michael Wagner are employees of Sanofi-Aventis and may hold shares and/or stock options in the company. Olof Eriksson, Iina Laitinen, Stefan Pierrou and Lars Johansson are employees of Antaros Medical AB. Philip J Larsen is an employee of Bayer Pharmaceuticals. Jan Erik Berglund is an employee of CTC AB. No other potential conflicts of interest relevant to this article exist.

KEY POINTS

QUESTION: Can GLP1R density in pancreas in individuals with T2D be evaluated by ^{68}Ga-Exendin4 PET?

PERTINENT FINDINGS: ^{68}Ga-Exendin4 binding in T2D pancreas was high, consistent with the known expression patterns of GlP1R in the abdominal area. GLP1R density correlated inversely with the age of the individual, and had a tendency to correlate positively to BMI.

IMPLICATIONS FOR PATIENT CARE: ^{68}Ga-Exendin4 PET may enable quantification of longitudinal changes of pancreatic GLP1R during the development in T2D and target occupancy in drug development studies.

REFERENCES

1. Andersen A, Lund A, Knop FK, Vilsbøll T. Glucagon-like peptide 1 in health and disease. Nat Rev Endocrinol. 2018 Jul;14(7):390-403.

2. Marso SP, Daniels GH, Brown-Frandsen K, Kristensen P, Mann JF, Nauck MA, Nissen SE, Pocock S, Poulter NR, Ravn LS, Steinberg WM, Stockner M, Zinman B, Bergenstal RM, Buse JB; LEADER Steering Committee; LEADER Trial Investigators. Liraglutide and Cardiovascular Outcomes in Type 2 Diabetes. N Engl J Med. 2016 Jul 28;375(4):311-22.

3. Marso SP, Bain SC, Consoli A, Eliaschewitz FG, Jódar E, Leiter LA, Lingvay I, Rosenstock J, Seufert J, Warren ML, Woo V, Hansen O, Holst AG, Pettersson J, Vilsbøll T; SUSTAIN-6 Investigators. Semaglutide and Cardiovascular Outcomes in Patients with Type 2 Diabetes. N Engl J Med. 2016 Nov 10;375(19):1834-1844. doi: 10.1056/NEJMoa1607141. Epub 2016 Sep 15. PMID: 27633186.

4. Eng J, Kleinman WA, Singh L, Singh G, Raufman JP. Isolation and characterization of exendin-4. an exendin-3 analogue. from Heloderma suspectum venom. Further evidence for an exendin receptor on dispersed acini from guinea pig pancreas. J Biol Chem. 1992 Apr 15;267(11):7402-5.

5. Selvaraju R, Velikyan I, Johansson L, Wu Z, Todorov I, Shively J, Kandeel F, Korsgren O, Eriksson O. In vivo imaging of the Glucagon Like Peptide-1 receptor in pancreas by [68Ga]DO3A-Exendin4. J Nucl Med. 2013 Aug;54(8):1458-63.

6. Boss M, Buitinga M, Jansen TJP, Brom M, Visser EP, Gotthardt M. PET-Based Human Dosimetry of 68Ga-NODAGA-Exendin-4. a Tracer for β-Cell Imaging. J Nucl Med. 2020 Jan;61(1):112-116.

7. Christ E, Wild D, Ederer S, Béhé M, Nicolas G, Caplin ME, Brändle M, Clerici T, Fischli S, Stettler C, Ell PJ, Seufert J, Gloor B, Perren A, Reubi JC, Forrer F. Glucagon-

like peptide-1 receptor imaging for the localisation of insulinomas: a prospective multicentre imaging study. Lancet Diabetes Endocrinol. 2013 Oct;1(2):115-22.

8. Eriksson O, Velikyan I, Selvaraju RK, Kandeel F, Johansson L, Antoni G, Eriksson B, Sörensen J, Korsgren O. Detection of Metastatic Insulinoma by Positron Emission Tomography with [68Ga]Exendin-4 - a case report. J Clin Endocrinol Metab. 2014;99:1519-24.

9. Tillner J, Posch MG, Wagner F, Teichert L, Hijazi Y, Einig C, Keil S, Haack T, Wagner M, Bossart M, Larsen PJ. A novel dual glucagon-like peptide and glucagon receptor agonist SAR425899: Results of randomized, placebo-controlled first-in-human and first-in-patient trials. Diabetes Obes Metab. 2019 Jan;21(1):120-128.

10. Frias JP, Nauck MA, Van J, Kutner ME, Cui X, Benson C, Urva S, Gimeno RE, Milicevic Z, Robins D, Haupt A. Efficacy and safety of LY3298176, a novel dual GIP and GLP-1 receptor agonist, in patients with type 2 diabetes: a randomised, placebo-controlled and active comparator-controlled phase 2 trial. Lancet. 2018 Nov 17;392(10160):2180-2193.

11. Brom M, Joosten L, Frielink C, Peeters H, Bos D, van Zanten M, Boerman O, Gotthardt M. Validation of 111In-Exendin SPECT for the Determination of the β-Cell Mass in BioBreeding Diabetes-Prone Rats. Diabetes. 2018 Oct;67(10):2012-2018.

12. Eriksson O, Haack T, Hijazzi Y, Teichert L, Tavernier V, Laitinen I, Berglund SE, Antoni G, Velikyan I, Johansson L, Pierrou S, Wagner M, Tillner J. Receptor occupancy of dual glucagon-like peptide 1/glucagon receptor agonist SAR425899 in individuals with type 2 diabetes mellitus. Sci Rep. 2020 Oct 7;10(1):16758.

13. Logan J, Fowler JS, Volkow ND, Wolf AP, Dewey SL, Schlyer DJ, MacGregor RR, Hitzemann R, Bendriem B, Gatley SJ. Graphical analysis of reversible radioligand binding

from time-activity measurements applied to [N-11C-methyl]-(-)-cocaine PET studies in human subjects. J Cereb Blood Flow Metab. 1990 Sep;10(5):740-7.

14. Patlak CS, Blasberg RG. Graphical evaluation of blood-to-brain transfer constants from multiple-time uptake data. Generalizations. J Cereb Blood Flow Metab. 1985 Dec;5(4):584-90.

15. Eriksson O, Velikyan I, Haack T, Hijazzi Y, Teichert L, Tavernier V, Berglund JE, Antoni G, Johansson L, Pierrou S, Wagner M, Tillner J. Hepatic binding, biodistribution and dosimetry of glucagon receptor PET tracer [68Ga]Ga-DO3A-VS-Tuna-2 in human subjects with type 2 diabetes. J Nucl Med. 2021;62:833-838.

16. Velikyan I, Rosenstrom U, Eriksson O. Fully automated GMP production of [68Ga]Ga-DO3A-VS-Cys40-Exendin-4 for clinical use. Am J Nucl Med Mol Imaging. 2017;7:111-125.

17. Göke R, Fehmann HC, Linn T, Schmidt H, Krause M, Eng J, Göke B. Exendin-4 is a high potency agonist and truncated exendin-(9-39)-amide an antagonist at the glucagon-like peptide 1-(7-36)-amide receptor of insulin-secreting beta-cells. J Biol Chem. 1993 Sep 15;268(26):19650-5.

18. Eriksson O, Rosenström U, Eriksson B, Velikyan I. Species differences in pancreatic binding of DO3A-VS-Cys40-Exendin4. Acta Diabetol. 2017;54:1039-1045.

19. Velikyan I, Bossart M, Haack T, Laitinen I, Larsen P, Evers A, Plettenburg O, Johansson L, Pierrou S, Wagner M, Eriksson O. First-in-class Positron Emission Tomography tracer for the Glucagon receptor. EJNMMI Res. 2019;9:17.

20. Eriksson O, Velikyan I, Haack T, Bossart M, Evers A, Laitinen I, Larsen PJ, Plettenburg O, Johansson L, Pierrou S, Wagner M. Drug occupancy assessment at the

Gastric Inhibitory Polypeptide (GIP) receptor by Positron Emission Tomography. Diabetes. 2021;70:842-853.

21. Wang L, Liu Y, Xu Y, Sheng J, Pan D, Wang X, Yan J, Yang R, Yang M. Age-related change of GLP-1R expression in rats can be detected by [18F]AlF-NOTA-MAL-Cys39-exendin-4. Brain Res. 2018 Nov 1;1698:213-219.

22. Kirk RK, Pyke C, von Herrath MG, Hasselby JP, Pedersen L, Mortensen PG, Knudsen LB, Coppieters K. Immunohistochemical assessment of glucagon-like peptide 1 receptor (GLP-1R) expression in the pancreas of patients with type 2 diabetes. Diabetes Obes Metab. 2017 May;19(5):705-712.

23. Kushner JA. The role of aging upon β cell turnover. J Clin Invest. 2013;123(3):990-995.

24. Wang X, Misawa R, Zielinski MC, Cowen P, Jo J, Periwal V, Ricordi C, Khan A, Szust J, Shen J, Millis JM, Witkowski P, Hara M. Regional differences in islet distribution in the human pancreas--preferential beta-cell loss in the head region in patients with type 2 diabetes. PLoS One. 2013 Jun 24;8(6):e67454.

25. Rahier J, Guiot Y, Goebbels RM, Sempoux C, Henquin JC. Pancreatic beta-cell mass in European subjects with type 2 diabetes. Diabetes Obes Metab. 2008 Nov;10 Suppl 4:32-42.

26. Khan M, Ouyang J, Perkins K, Nair S, Joseph F. Determining predictors of early response to exenatide in patients with type 2 diabetes mellitus. J Diabetes Res. 2015;2015:162718.

27. Athauda D, Maclagan K, Skene SS, Bajwa-Joseph M, Letchford D, Chowdhury K, Hibbert S, Budnik N, Zampedri L, Dickson J, Li Y, Aviles-Olmos I, Warner TT, Limousin P, Lees AJ, Greig NH, Tebbs S, Foltynie T. Exenatide once weekly versus placebo in

Parkinson's disease: a randomised, double-blind, placebo-controlled trial. Lancet. 2017 Oct 7;390(10103):1664-1675.

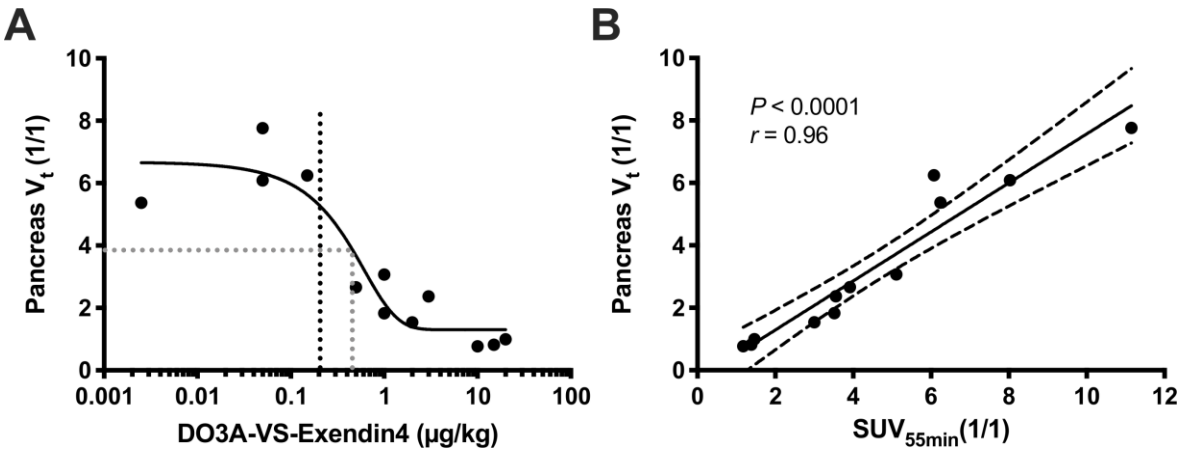

Figure 1. In vivo binding of ^{68}Ga-Exendin4 in NHP pancreas. Dose escalation studies demonstrated strong binding in pancreas at mass doses below 0.2 µg/kg (black dotted line), which was progressively blocked by co-injection of increasing amounts of unlabeled DO3A-VS-Exendin4 precursor peptide (A). The 50% blocking dose is indicated by a grey dotted line. There was a strong correlation between the V_t (obtained from a dynamic 90 minutes scan and requiring a blood plasma input signal) and the SUV_{55min} values, indicating the just a static scan from 50-60 minutes can replace a dynamic scan (B).

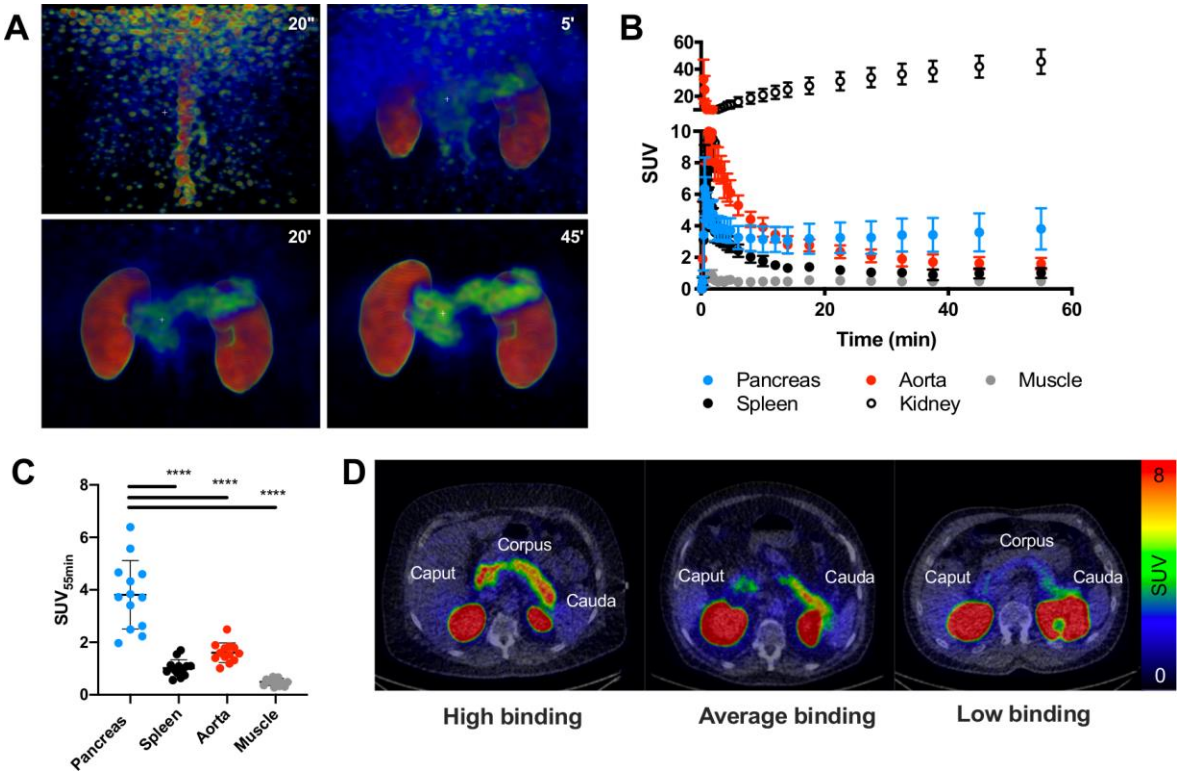

Figure 2. Abdominal biodistribution of ^{68}Ga-Exendin4 in humans with T2D. ^{68}Ga-Exendin4 was rapidly distributed followed by washout from most tissues except pancreas and kidneys (A and B, average of n=13 individuals). Representative maximum intensity projection (MIP) PET images are shown. There was strong variability in the pancreas binding, which was not reflected in other tissues (C). Representative transaxial PET/CT images demonstrating high (left panel), average (middle panel) or low (right panel) pancreas binding of ^{68}Ga-Exendin4 (D). The approximate surgical segment of the pancreas (caput=head, corpus=body, cauda=tail) is given as adjacent white text.

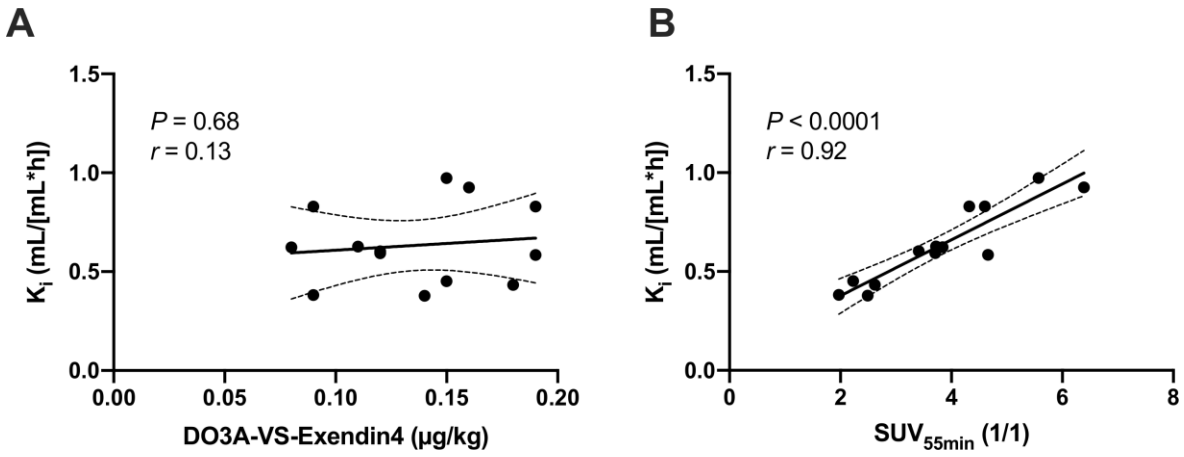

Figure 3. In vivo binding of ^{68}Ga-Exendin4 in human T2D pancreas. There was no obvious self-blocking mass effect at peptide doses below 0.2 µg/kg (i.e. no negative correlation) (A). In human pancreas, there was a strong correlation between the model parameter obtained from a dynamic scan including blood (Patlak K_i) and the SUV_{55min} values, indicating that a static scan is sufficient for accurate quantification (B).

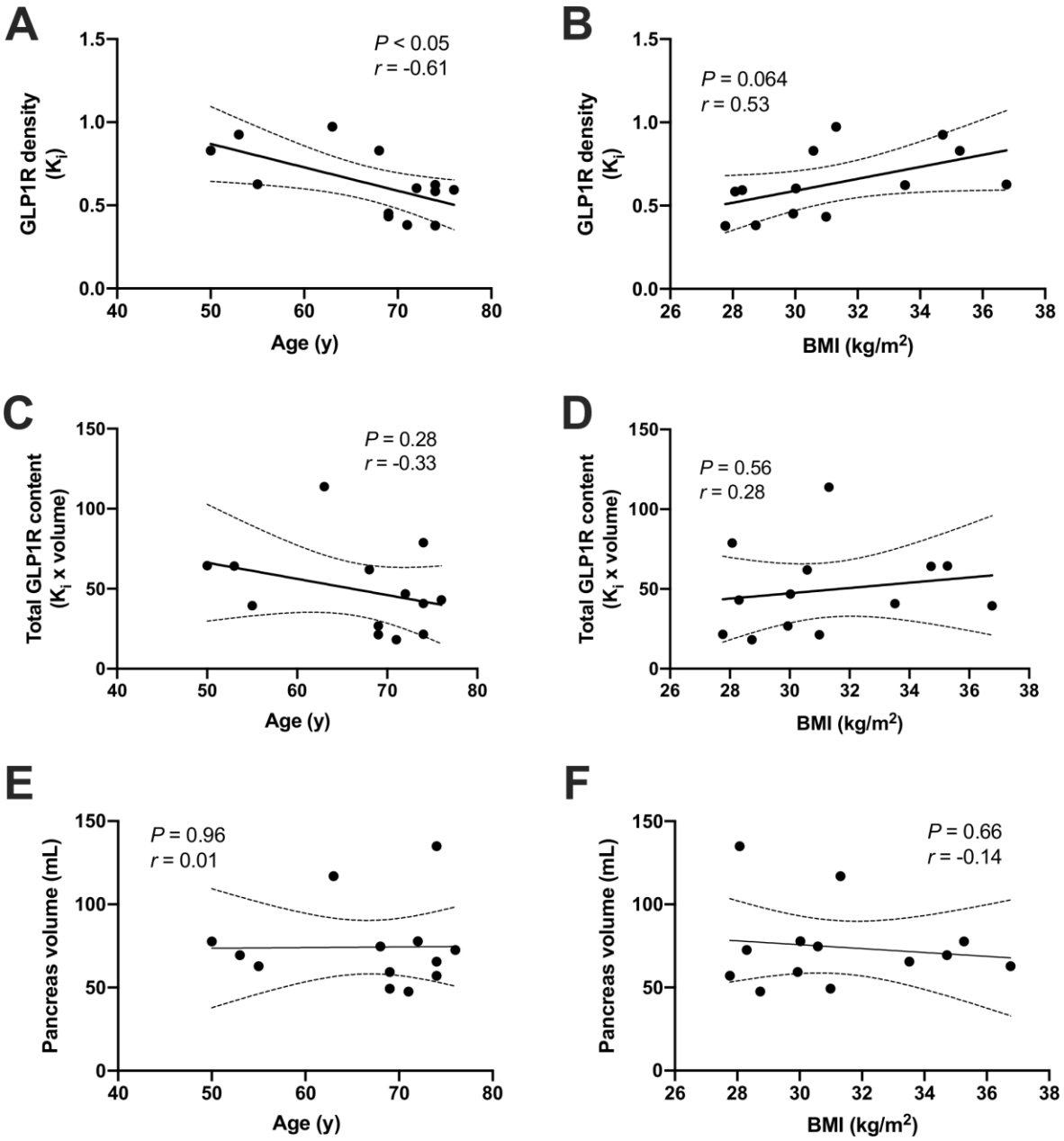

Figure 4. Correlation of ^{68}Ga-Exendin4 pancreas binding to biometric parameters. The pancreatic GLP1R density (concentration of ^{68}Ga-Exendin4 binding) correlated negatively to the age of the examined individuals (A), and also exhibited a tendency to correlate to the BMI (p=0.064) (B). However, the total pancreas GLP1R content (i.e. ^{68}Ga-Exendin4 concentration multiplies with volume) did not correlate with age (C) nor BMI (D) of the participants. Similarly, the size of the pancreas did not correlate to either the age (E) nor the BMI (F) in this study.

TABLES

Table 1. Overview of dose escalation of ^{68}Ga-Exendin4 and co-injected DO3A-VS-Exendin4 in NHPs. NHP experiments #2 and #5 were performed in the same individual 6 months apart.

ID		NHP 1	NHP 2	NHP 3	NHP 4	NHP 5
	Weight (kg)	5.6	5.5	7.4	9.0	6.0
Scan 1	µg/kg	2	0.05	0.15	0.05	0.0025
	MBq	11.1	2.0	4.6	2.3	0.2
Scan 2	µg/kg	-	1	20	1	0.5
	MBq	-	6.5	11.1	6.7	6.9
Scan 3	µg/kg	-	10	-	3	15
	MBq	-	5.2	-	4.9	18.7

Table 2. Metabolic stability and blood plasma ratio of ^{68}Ga-Exendin4 in individuals with T2D (n=3).

Time (min)	Intact peptide (%)	Plasma-to-blood ratio (1/1)
5	98.1±0.9	1.76±0.06
30	95.2±0.4	1.80±0.05
60	90.1±1.4	1.79±0.05

Table 3. Patlak graphical analysis K_i net uptake rat and goodness-of-fit for all individuals examined with ^{68}Ga-Exendin4. Table also includes with SUV_{55min} values and pancreas volumes in the same individuals for comparison.

Individual	Volume (mL)	SUV_{55min} (1/1)	K_i (mL/[mL*h])	R^2
1	78	3.4	0.60	0.99
2	69	6.4	0.93	1.0
3	48	2.0	0.38	0.97
4	66	3.8	0.62	0.98
5	63	3.7	0.63	0.98
6	78	4.3	0.83	0.99
7	59	2.2	0.45	0.99
8	73	3.7	0.59	1.0
9	57	2.5	0.38	0.99
10	49	2.6	0.43	0.97
11	75	4.6	0.83	0.99
12	135	4.7	0.58	0.99
13	117	5.6	0.97	1.0

GRAPHICAL ABSTRACT

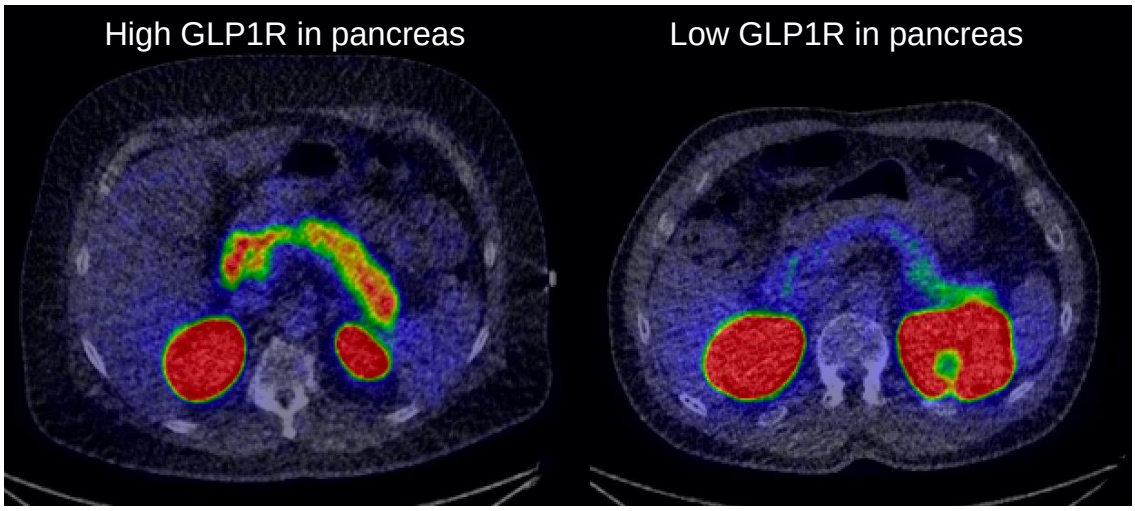

Supplementary data, Glucagon Like Peptide-1 receptor imaging in individuals with Type 2 Diabetes

METHODS AND MATERIALS

In vitro binding specificity and internalization assays

The binding specificity and internalization characteristics of the GMP batch of DO3A-VS-Exendin4 used in this study was examined in vitro. The binding specificity was assessed using an in vitro autoradiography binding assay, using frozen sections of relevant cell lines. ^{68}Ga-Exendin4 at a concentration of 5 nM was incubated with frozen sections of pellets of HEK293 cells, transfected either with human GLP1R or human Gastric Inhibitory Polypeptide receptor (GIPR) as described previously (*1*), as well as sections from INS-1 insulinoma explanted mice xenograft tumors (*2*). GIPR overexpressing cells were used to rule out any cross reactivity of ^{68}Ga-Exendin4 to GIPR, which is related to GLP1R and also expressed in pancreas. INS-1 cells derived from rat beta cells and known to express GLP1R (*2*).

Sections were incubated with either ^{68}Ga-Exendin4 alone, or co-incubated with with 1μM GLP1(7-36), 10μM glucagon or 1μM unlabeled DO3A-VS-Exendin4. Sections were incubated at room temperature (RT) for 60 minutes in PBS containing 1% Bovine Serum Albumin (pH 7.4). Next, the sections were washed 1 x 1 min in assay buffer and 2 x 1 in in PBS followed by airdrying at 37ºC. The sections were then exposed to a phosphor-imager screen overnight and digitalized using a Cyclone Phosphor Imager system (PerkinElmer). Autoradiogram images were visualized using ImageJ (NIH, US).

The cell internalization assay was performed as described in detail previously (*3*). Briefly, HEK293 cells transfected with human GLP1R (approximately 300.000 cells) were incubated with 10 nM ^{68}Ga-Exendin4 in complete media for up to 120 minutes, either at RT or at 4 °C. To measure membrane bound and internalized radioligand, cells were treated with 0.2 M glycine buffer containing 4 M urea (pH 2.5) (acid wash buffer) for 5 minutes and the supernatant (containing the membrane bound fraction) measured in a gamma counter. Next, the cells were treated with 1 M NaOH (basic wash buffer) for 30 minutes and the detached cells were measured by gamma counter (internalized fraction).

The assay was repeated three times. The total and internalized fraction of ^{68}Ga-Exendin4 at RT or at 4 °C was analyzed using Excel.

In vivo metabolic stability

Blood samples were centrifuged at 4000 rpm for 2 minutes at 4°C (Beckman Allegra X-22R Centrifuge, Palo Alto, USA). From the plasma 0.5 ml was taken and an equal volume of acetonitrile was added to precipitate the proteins. The mixture was centrifuged at 13200 rpm at 4 °C for 1 min at 4 °C (Eppendorf 5415R centrifuge, Eppendorf AG, Hamburg, Germany). The supernatant was filtered through a 0.2µm nylon membrane (Corning Incorporated, Corning, NY, USA) by centrifugation at 13200 rpm at 4°C for 1 min. Five hundred µl of the filtered supernatant was diluted with 1500µl deionized water, and then 30µl 0.01mM of unlabeled DO3A-VS-Exendin-4 was added to the mixture. The sample preparation recovery was determined by measuring the radioactivity in the plasma, filters and pellet.

High performance liquid chromatography (HPLC) analysis was performed using a binary pump system (Gilson, Middleton, USA). The sample (1.8 ml) was injected using an automated solid phase extraction controller (ASPEC Gilson) connected to a dilutor (Gilson). The separation was performed on a Xbridge Prep BEH130 C18 chromatographic column (peptide separation technology, 250mm x 10mm i.d 5µm) with a 10x10 mm C18 security guard from the same supplier. The HPLC system was operated at a flow rate of 6 ml/min. The mobile phase consisted of 0.1% TFA in MilliQ: 0.1% TFA in Acetonitrile. Gradient elution mode was used for the separation (Gradient: 0-7 min: 5-70%, 7-12 min: 70%, 12-13 min: 70-5%, 13-15 min: 5%)

A second method was developed with a slower gradient, to determine if any radioactive metabolites were co-eluting with the DO3A-VS-Exendin-4 peak. A UV detector (Gilson) was used to detect unlabeled DO3A-VS-Exendin-4 at 220nm. The outlet from the detector was connected to a switching valve on the arm of the ASPEC to enable automatic fraction collection. Six fractions were collected and the radioactivity in the fractions was measured by a well-type scintillation counter. A radio detector (Radiomatic 610TR, Packard, USA) was coupled in series with the UV detector.

RESULTS

In vitro binding specificity and internalization assays

The GMP batch of ^{68}Ga-Exendin4 bound to huGLP1R-HEK293 cells, but not huGIPR-HEK293 cells (Supplementary Figure 1). The binding to huGLP1R-HEK293 cells could be inhibited by co-incubation with GLP1(7-36) and unlabeled DO3A-VS-Exendin4, but not glucagon. Similarly, ^{68}Ga-Exendin4 bound to insulinoma model INS-1 sections, again abolished by GLP-1 agonists but not glucagon. ^{68}Ga-Exendin4 demonstrated rapid binding and approximately 50% internalization to viable huGLP1R-HEK293 cells. The internalization could be arrested by decreased temperature, indicating that it was an active process.

FIGURES AND TABLES

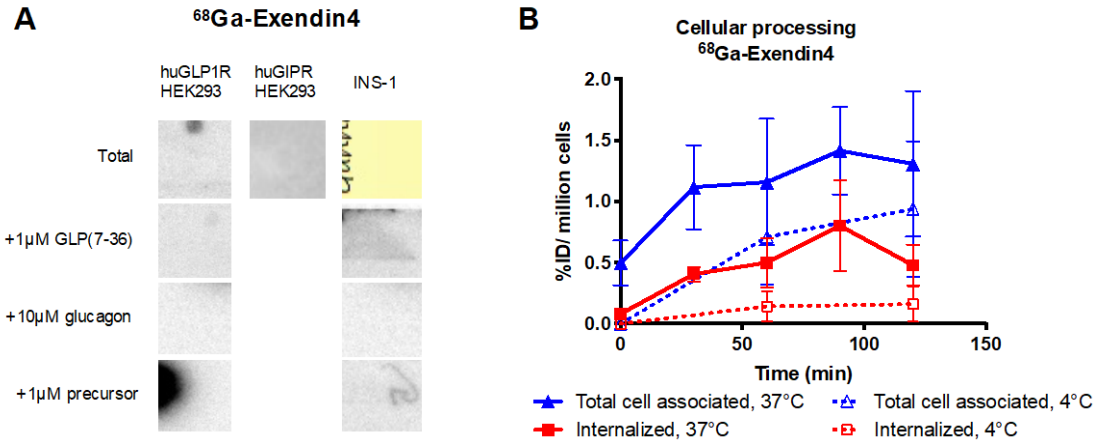

Supplementary Figure 1. In vitro ^{68}Ga-Exendin4 binding characteristics. ^{68}Ga-Exendin4 binding specificity assessed by in vitro frozen section autoradiography (A) and internalization assessed in viable huGLP1R-HEK293 cells (B).

Supplementary Table 1. Compartment model (1TC) parameters and goodness-of-fit for all individuals examined with ^{68}Ga-Exendin4.

1TC				
Subject	**K_1**	**k_2**	**V_a**	**R_2**
1	0.41	1.51	0.02	0.24
3	0.37	1.33	0	0.69
2	0.05	0.04	0.15	-0.03
4	0.03	0.04	0.11	-0.04
5	0.28	1.02	0.05	0.11
7	0.69	2.57	0.01	0.72
9	0.21	1.01	0.07	0.68
10	0.03	0.07	0.12	0.56
6	0.28	0.86	0.06	0.25
8	0.05	0.07	0.12	0.03
12	0.14	0.39	0.05	-0.18
11	0.07	0.08	0.09	-0.45
13	0.05	0.04	0.11	0.12
Average	**0.2**	**0.7**	**0.07**	**0.21**
StDev	**0.19**	**0.75**	**0.05**	**0.35**

Supplementary Table 2. Compartment model (2TCk3, i.e. no k4) parameters and goodness-of-fit for all individuals examined with ^{68}Ga-Exendin4.

2TCk3					
Subject	**K_1**	**k_2**	**k_3**	**V_a**	**R_2**
1	0.53	2.33	0.05	0.01	0.97
3	0.42	1.69	0.03	0	0.95
2	0.76	3	0.07	0.02	0.88
4	0.52	3	0.07	0.03	0.96
5	0.44	2.16	0.06	0.04	0.95
7	0.74	3	0.03	0	0.96
9	0.33	2	0.05	0.06	0.98
10	0.3	2.27	0.07	0.08	0.92
6	0.44	1.83	0.06	0.04	0.96
8	0.42	1.95	0.05	0.03	0.96
12	0.38	1.77	0.06	0.01	0.93
11	0.55	2.41	0.07	0.01	0.92
13	0.52	2.47	0.1	0.01	0.9
Average	**0.49**	**2.3**	**0.06**	**0.03**	**0.94**
StDev	**0.13**	**0.45**	**0.02**	**0.02**	**0.03**

Supplementary Table 3. Compartment model (2TC) parameters and goodness-of-fit for all individuals examined with ^{68}Ga-Exendin4.

2TC						
Subject	**K_1**	**k_2**	**k_3**	**k_4**	**V_a**	**R^2**
1	0.55	2.54	0.17	0.18	0.01	0.96
3	0.42	1.74	0.09	0.16	0	0.94
2	0.75	3	0.08	0.01	0.02	0.88
4	0.51	3	0.08	0.01	0.03	0.96
5	0.45	2.22	0.07	0	0.04	0.95
7	0.73	3	0.04	0.01	0	0.96
9	0.34	2.07	0.05	0.01	0.06	0.98
10	0.34	2.73	0.1	0.02	0.07	0.93
6	0.44	1.87	0.07	0	0.04	0.96
8	0.42	1.98	0.06	0	0.03	0.96
12	0.4	1.95	0.07	0.01	0.01	0.95
11	0.59	2.66	0.1	0.01	0.01	0.94
13	0.59	3	0.14	0.01	0.01	0.94
Average	0.02	0.03	0.08	2.44	0.5	0.95
StDev	0.18	0.8	0.03	0.65	0.13	0.02

Supplementary Table 4. Patlak graphical analysis parameters and goodness-of-fit for all individuals examined with ^{68}Ga-Exendin4.

Patlak		
Subject	K_i (mL/mL/s)	R^2
1	0.00017	0.99
3	0.00011	0.97
2	0.00026	1
4	0.00017	0.98
5	0.00017	0.98
7	0.00013	0.99
9	0.0001	0.99
10	0.00012	0.97
6	0.00023	0.99
8	0.00016	1
12	0.00016	0.99
11	0.00023	0.99
13	0.00027	1
Average	0.00018	**0.99**
StDev	0.00005	**0.01**

Supplementary Table 5. Logan graphical analysis parameters and goodness-of-fit for all individuals examined with ^{68}Ga-Exendin4.

Logan		
Subject	V_t	R^2
1	0.76	0.99
3	0.53	0.99
2	1.4	0.99
4	0.79	0.96
5	0.97	0.98
7	0.63	0.99
9	0.5	0.97
10	0.56	0.97
6	1.11	0.81
8	0.81	0.98
12	0.91	1
11	1.15	0.98
13	1.41	0.98
Average	0.89	**0.97**
StDev	0.3	**0.05**

REFERENCES

1. Eriksson O, Velikyan I, Haack T, et al. Drug occupancy assessment at the Gastric Inhibitory Polypeptide (GIP) receptor by Positron Emission Tomography. *Diabetes*. 2021;70:842-853.

2. Selvaraju RK, Velikyan I, Asplund V, et al. Pre-clinical Evaluation of [68Ga]Ga-DO3A-VS-Cys40-Exendin-4 For Imaging of Insulinoma. *Nucl med biol*. 2014;41:471-6.

3. Velikyan I, Bossart M, Haack T, et al. First-in-class Positron Emission Tomography tracer for the Glucagon receptor. *EJNMMI res*. 2019;9:17.